

# Study of plastic scintillator based reactor neutrino detector

|                              |  |
|------------------------------|--|
| 著者(英語)                       | Hiroaki Ono, Katsuyuki Takahashi, Hitoshi Miyata, Kyouhei Ishida, Masaaki Katsumata, Minori Watanabe |
| journal or publication title | Bulletin of the Nippon Dental University.<br>General education                                       |
| volume                       | 41   |
| page range                   | 25-30  |
| year                         | 2012-03-20   |
| URL                          | <a href="http://doi.org/10.14983/00000061">http://doi.org/10.14983/00000061</a>                      |

# Study of Plastic Scintillator based Reactor Neutrino Detector

Hiroaki Ono<sup>1</sup>, Katsuyuki Takahashi<sup>2</sup>, Hitoshi Miyata<sup>3</sup>, Kyouhei Ishida<sup>2</sup>,  
Masaaki Katsumata<sup>3</sup>, Minori Watanabe<sup>2</sup>

<sup>1</sup>Nippon Dental University School of Life Dentistry at Niigata, 1-8 Hamaura-cho Chuo-ku, Niigata, Niigata, Japan

<sup>2</sup>Graduate School of Science and Technology, Niigata University, 8050 Ikarashi 2-no-cho, Nishi-ku, Niigata, Niigata, Japan

<sup>3</sup>Faculty of Science Physics Department, Niigata University, 8050 Ikarashi 2-no-cho Nishi-ku, Niigata, Niigata, Japan

Dated: 8 February 2012

## Abstract

Recently nuclear power plant becomes one of the important electric power sources to reduce the greenhouse gasses emission. Nuclear reactor fuel consists of the uranium-235 (<sup>235</sup>U) enriched uranium and produces the thermal energy via nuclear fission process. Through the reactor operation, uranium-238 (<sup>238</sup>U) fission also produces the plutonium- 239 (<sup>239</sup>Pu), which should be strictly under controlled to avoid the diversion to the nuclear weapon for a nonproliferation and safeguard. At this point, monitoring of the nuclear power plant operation and its fuels exchange have important role for the peaceful nuclear energy usage. In this study, we produce the prototype of nuclear reactor monitor based on the plastic scintillator detecting anti-neutrinos, which produced through the several times of beta-decay from the nuclear fission products. In addition, we apply the monitoring performance simulation assuming the 1 ton size detector placed very closely to the reactor core.

Key words: Gadolinium loaded plastic scintillator, Reactor neutrino detector, Reactor monitor

## 1. Introduction

Neutrino was discovered by F. Reines and C. L. Cowan in 1953 ~ 19590[1] and the nuclear reactor was used as a source of neutrino at that time. From the first observation of the neutrino, nuclear reactor is used as a source of anti-neutrino ( $\bar{\nu}_e$ ) induced from the nuclear fission process.

Fresh nuclear fuel is composed of the uranium-235 enriched uranium-oxide pellet; <sup>235</sup>U (3~5%) and <sup>238</sup>U (95~97%) as shown in Figure 1, and generates 200 MeV of thermal energy from the nuclear fission process. Decay products produced from the uranium nuclear fission emit the anti-neutrinos via beta-decay processes until unstable radioactive products become stable.

Through the reactor operation cycle, plutonium is produced from the uranium fuel burn-up through the following nuclear fission process:

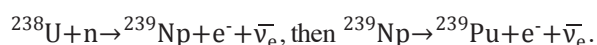


Figure 1 also shows the constituent ratio of the spent nuclear fuel after the operation cycle and ~1% of <sup>239</sup>Pu will exist in the spent fuel. Since plutonium isotope can easily extract and purify via chemical process, plutonium inventory should be strictly controlled to restrict the diversion to the nuclear weapon.

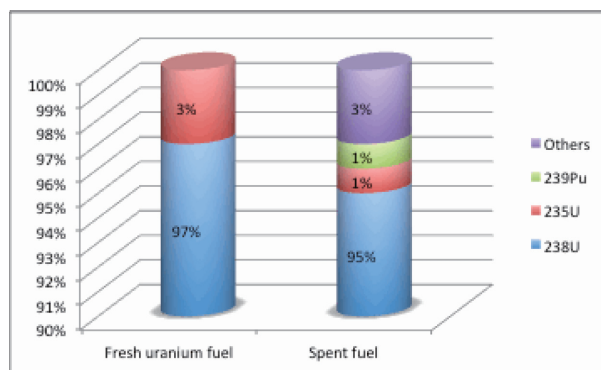


Figure 1 Composition ratio of the nuclear fuel components before and after the reactor operation cycle.

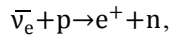
From the safeguards point of view, reactor neutrino detector comes up as an integrated application of the reactor operation and nuclear fuel monitor using the large amount of penetrating anti-neutrinos, which is required by International Atomic Energy Agency (IAEA)[1].

Commercial nuclear power plants (3 GW in thermal power) produce the large amount of anti-neutrinos ( $2 \times 10^{20} \bar{\nu}_e/s$ ), thus many reactor neutrino experiments use the nuclear power plant as a source of anti-neutrino. Recent reactor neutrino detector is based on the gadolinium (Gd) doped liquid scintillator in order to achieve the large volume of anti-neutrino target, since anti-neutrino is detected via inverse-beta-decay reaction,  $\bar{\nu}_e + p \rightarrow e^+ + n$ , thus detector material should be composed of the large amount of hydrogen nucleus and also have a capability to detect the neutron signal efficiently.

However, liquid scintillator is based on the flammable mineral oil and it will be difficult to place the inflammable objects very closely to the reactor core from a reactor operation safety point of view, even the number of detected neutrinos increase inversely with the square of the distance. In this situation, we propose the new reactor monitor composed of the Gd-doped plastic scintillator. Since plastic scintillator is based on the non-flammable stable material involving the hydrogen nucleus, we will have a capability to locate near the reactor core. On the other hand, Gd-loaded plastic scintillator is not commercially available at this moment. Therefore we develop the Gd-loaded plastic scintillator cooperating with the company.

## 2. Anti-neutrino Detection Method

Reactor anti-neutrino is detected via the inverse-beta-decay reaction between the anti-neutrino and the hydrogen nucleus in the scintillator:



then produce the positron ( $e^+$ ) and neutron ( $n$ ).

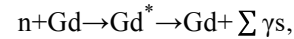
In order to increase the detection efficiency of the neutrons, 0.1% of Gd is doped into the scintillator in a unit of weight, since Gd ( $^{155}\text{Gd}$  and  $^{157}\text{Gd}$ ) has largest reaction cross-section to the thermal neutrons. Figure 2 shows the detection scheme of the anti-neutrinos via inverse-beta-decay process. Produced positron deposits its energy and finally annihilates with the

electron and emits the two  $\gamma$ -rays, whose energy sum becomes 1.02 MeV. From the inverse-beta-decay reaction, we obtain the anti-neutrino energy  $E_{\bar{\nu}}$  as:

$$E_{\bar{\nu}} = E_{e^+} + (M_n - M_p) \sim E_{\text{vis}} + 1.8 \text{ MeV},$$

where  $E_{e^+}$  and  $E_{\text{vis}}$  are positron total energy and visible energy measured as prompt signal.  $M_n - M_p$  is a mass difference between the neutron and proton. Considering the positron mass and nucleon mass difference, anti-neutrino energy threshold becomes 1.8 MeV and we can extract the anti-neutrino energy from the measured visible energy.

On the other hand, generated neutron collides with the protons several times and gradually thermalized, then absorbed with Gd and immediately emits the several  $\gamma$ -rays with following reaction;



whose energy sum becomes 8 MeV in total. Thermalized neutron travels in the scintillator material around 30  $\mu\text{s}$  in average until absorbed with Gd (0.1%/w), thus we observe the correlated signal delayed from the positron detection timing with the energy sum of 8 MeV from the n-Gd capture reaction.

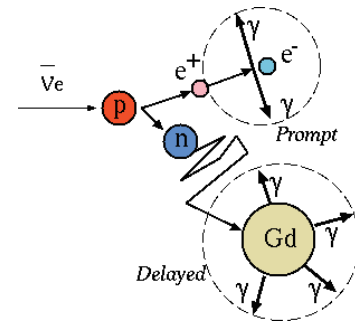


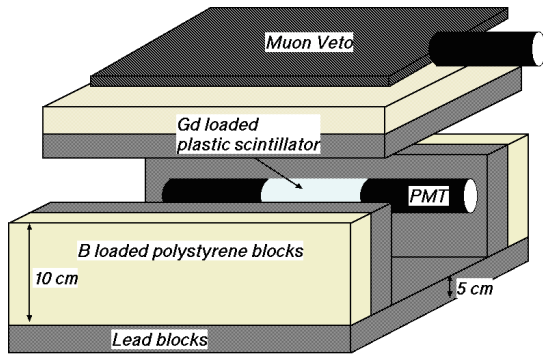
**Figure 2** Anti-neutrino detection via inverse-beta-decay reaction with the delayed coincidence method.

To identify the anti-neutrino event and suppress the accidental backgrounds, we use the delayed coincidence method: require the coincidence between the positron prompt signal and n-Gd captured delayed signal within the 50  $\mu\text{s}$ . We also require the higher energy sum for the delayed candidate signal corresponding to the n-Gd capture signal.

## 3. Bench-test of Test Sample

To avoid the difficulty of placing Gd-doped liquid

scintillator detector very closely to the reactor core for the fire safety concern, we develop the Gd-loaded plastic scintillator even that is not commercially available at this moment. Plastic scintillator company Kuraray succeed to develop the Gd-doped plastic scintillator test sample; 22 cm-length, 2 inch- $\phi$  with doping the 0.1% of Gd in a unit of weight. Emitted scintillator light are transport to the both ends of the scintillator and read out by photo-multiplier tube (PMT). We attach the Hamamatsu H7195 2-inch PMT for both ends of scintillator sample and convert the scintillation light into the photo-electrons amplified to be  $10^6$ . Finally we read out the PMT analog outputs with REPIC RPV-171 16-channel, 12-bit VMEADC (0.25 pC/count) converted to the digital data (ADC count) and 16-channel, 52  $\mu$ s dynamic range of CAEN V1290N VME multihit-TDC (25 ps time resolution) to record the time difference between the prompt and delayed signal. Each VME module is controlled with the Sanriz SVA-041 VME board computer.



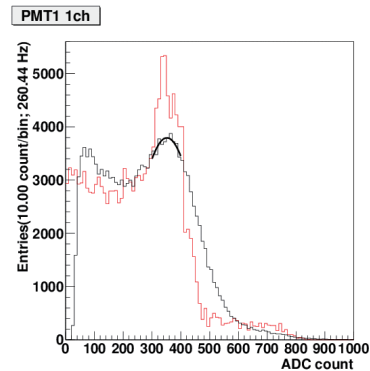
**Figure 3** Bench-test setup to measure the Gd-loaded plastic scintillator test sample.

Figure 3 shows the whole bench test setup of the Gd-loaded plastic scintillator sample with Am/Be pseudo neutrion event. Concerning the environmental backgrounds, scintillator sample is surrounded by the 5 cm-thick of lead and boron-loaded polyethylene blocks to reduce the contribution from the environmental radiation or neutrons mainly produced through the muon nuclear spallation.

On the top side, we put the 43 cm  $\times$  55 cm 3 mm-thick of muon-veto counter to suppress the cosmic muon background. We set the 200  $\mu$ s of veto-time after coming the muon signal for the muon-veto counter.

With this setup, we calibrate the Gd-loaded plastic

scintillator with  $^{60}\text{Co}$   $\gamma$ -rays (1.173 and 1.332 MeV) source. Since scintillator size is not enough to confine the all  $\gamma$ -rays, we only observe the compton scattering signal from the  $\gamma$ -rays. In addition, this prototype detector does not have enough resolution to separate each  $\gamma$ -ray compton-edge (0.96 and 1.12 MeV), we determin the measured ADC edge position as 1.04 MeV, which is a mean value of the two compton-edge energies, as shown Figure 4.



**Figure 4** Energy calibration with  $^{60}\text{Co}$   $\gamma$ -ray source for experimental data (black) and simulation (red).

Finally we obtain the calibration factor as 352 counts/MeV by fitting the compton-edge peak position. In Figure 4, we also plot the simulated energy distribution with assuming the same scintillator size but without considering energy resolution. After calibrating all the PMTs, we proceed to measure the pseudo anti-neutrino signal with Am/Be neutron source.

## 4. Background Study

Before measuring the pseudo anti-neutrino signal with Am/Be source, we evaluate the environmental radiation background with 3 inch- $\phi$  NaI(Tl) scintillation counter. Figure 5 shows the energy distribution measured with NaI counter after calibrating the  $^{60}\text{Co}$   $\gamma$ -ray source. From the Figure 5, we observe the three major peaks, which come from the following radioisotopes:  $^{40}\text{K}$  (1.46 MeV),  $^{214}\text{Bi}$  (1.76 MeV) and  $^{208}\text{Tl}$  (2.6 MeV), laid on the flat muon background, which is estimated from the other experimental result [3].

Since these environmental radiations must be a background for the prompt signal, it is desired to apply the cut for the prompt energy:  $E_{\text{prompt}} > 2.6$  MeV, to be free from the

environmental radiation backgrounds.

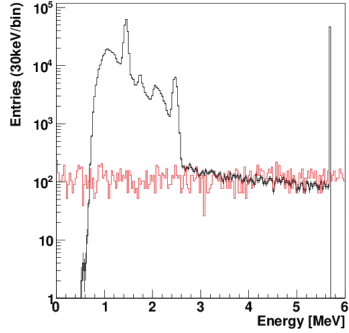


**Figure 5** Environmental background measured with NaI(Tl) scintillation counter (black) and expected muon background measured at BESS experiment [3].

## 5. Pseudo Experiment with Am/Be

For the bench test of the prototype detector, we use the Am/Be neutron radioactive source as a pseudo signal of the anti-neutrino event. Am/Be neutron source emits the correlated  $\gamma$ -ray and neutron via the following process:  $\alpha + {}^9_4\text{Be} \rightarrow n + {}^{12}_6\text{C}^*$ , where americium emits the  $\alpha$ -ray ( ${}^{241}_{95}\text{Am} \rightarrow \alpha + {}^{237}_{93}\text{Np}$ ) and absorbed with the beryllium target, then decays into the neutron and the excited state of carbon, which immediately emits the 4.3 MeV of monochrome energy  $\gamma$ -ray.

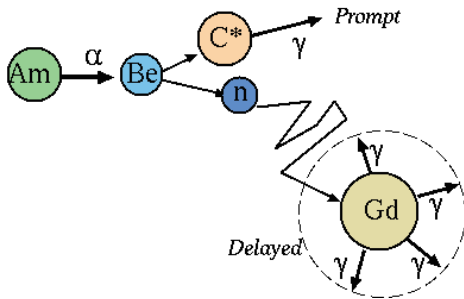


**Figure 6** Pseudo anti-neutrino event with Am/Be neutron source.

With these correlated signal between the  $\gamma$ -ray and neutron, we use the Am/Be as a source of the pseudo anti-neutrino event, where  $\gamma$ -ray is a prompt signal instead of the positron and neutron capture signal becomes delayed signal in the pseudo inverse beta-decay process, as shown in Figure 6. In

order to suppress the environmental backgrounds, we use the delayed coincidence method and require the coincidence between prompt and delayed signals after coming the 2 to 52  $\mu\text{s}$  time window, called On-timing data using multi-hit TDC data. We also take the same 50  $\mu\text{s}$  window size but different timing corresponding to the correlated backgrounds what comes after 600  $\mu\text{s}$  from prompt signal, called Off-timing data.

**Figure 7** shows the energy distribution of the prompt and delayed candidates for both On- (gray) and Off-timing (red) data taking with the Am/Be pseudo anti-neutrino source. To suppress the background from the environmental radiation, we apply the following cuts for the prompt and delayed signals: Prompt:  $2.6 < E_{\text{delayed}} < 7.7$  MeV, Delayed:  $5.5 < E_{\text{prompt}} < 7$  MeV, where  $E_{\text{prompt}}$  and  $E_{\text{delayed}}$  denote the energy sum of the prompt and delayed signal.

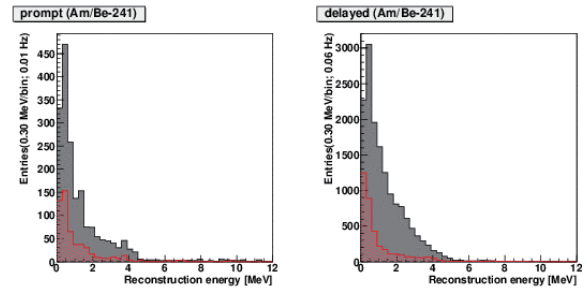


**Figure 7** Energy distributions of the prompt (left) and delayed (right) signal with the Am/Be source for On- (red) and Off-timing (gray) data.

From these cuts, we select the 4.3 MeV of  $\gamma$ -ray signal as prompt candidate and n-Gd capture  $\gamma$ -ray signal as delayed candidate. Since our detector cannot confine the all  $\gamma$ -rays produced via positron or n-Gd captured process, there is no significant peak in both prompt and delayed energy distribution in **Figure 7**.

With these cuts condition, we obtain the candidate of pseudo signal of the anti-neutrino and apply the fitting to the time difference distribution after subtracting the Off-timing background contribution. Finally we obtain the mean neutron capture time of  $23.7 \pm 3.8$   $\mu\text{s}$  with the Gd-loaded plastic scintillator test sample, as shown in **Figure 8**.

Considering 0.1%/W Gd composition, we will obtain the  $\sim 30$   $\mu\text{s}$  mean capture time from the other experiment [4], we expect to observe the n-Gd captured signal and obtain the

pseudo anti-neutrino candidates with Gd-loaded plastic scintillator.

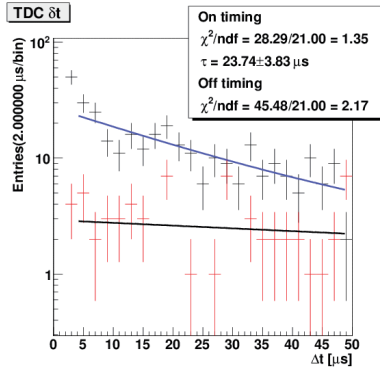


**Figure 8** Time difference ( $\Delta t$ ) distribution between the prompt and delayed signals with Am/Be both On- (black) and Off-timing (red).

### 6. Large Prototype Detector Simulation

For monitoring reactor fuel exchange cycle, we assume the 1 m<sup>3</sup>, 1 ton size of prototype detector composed of the Gd-doped plastic scintillator located at the commercial reactor (3.3 GWth) very close to the reactor core. (25 m).

**Figure 9** shows simulation results of the expected energy distributions of prompt and delayed signal by anti-neutrino inverse-beta-decay reaction in the 1 ton size detector.

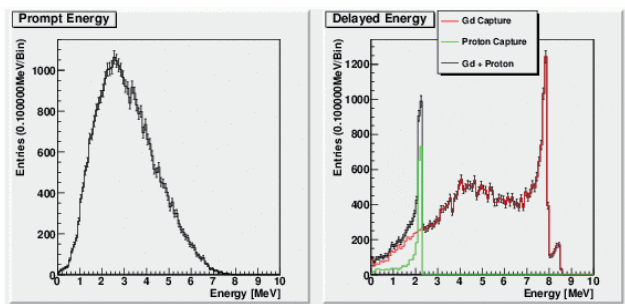


**Figure 9** Simulated energy distribution of prompt (left) and delayed (right) with assuming the 1 t size detector.

Prompt signal has peak around the 2.5 MeV from the positron related signal. Delayed signal has two main peaks produced from the n-p or n-Gd capture processes, which emit the 2.2 MeV or 8 MeV of  $\gamma$ -rays in total, respectively.

Background contributions are also estimated scaling the

results measured with NaI discussed at Sec. 4 and summarized in Table 1.

Table 1 Estimated background rate for 1 ton prototype scaled from the NaI measurement.

| BG source                    | Rate                            |
|------------------------------|---------------------------------|
| <sup>40</sup> K (1.46 MeV)   | 16 kHz                          |
| <sup>214</sup> Bi (1.76 MeV) | 9.1 kHz                         |
| <sup>208</sup> Tl (2.61 MeV) | 41 kHz                          |
| Muon                         | 0.22 Hz (scaled from SONGS [5]) |

Environmental radiation background has 2.6 MeV peak from the <sup>208</sup>Tl as maximum, we optimize the cut position to achieve the maximum signal to noise ratio (S/N). With optimizing the cut position, we obtain the maximum S/N with  $E_{\text{prompt}} > 2.7$  MeV, as shown in Figure 10. Finally we select the cut position for prompt:  $2.7 < E_{\text{prompt}} < 8$  MeV and delayed:  $2.7 < E_{\text{delayd}} < 8.5$  MeV. We also apply the time difference cut as  $11 < \tau < 50 \mu\text{s}$  to remove the muon decay events in the detector.

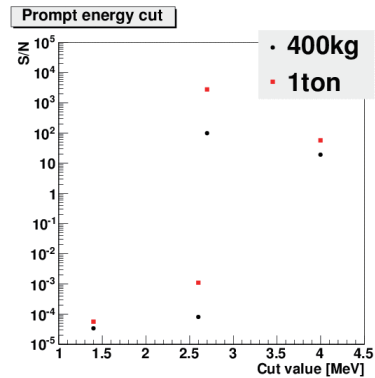


**Figure 10** S/N ratio with prompt energy cut with assuming the large detector volume design

With these cuts condition, we expect to obtain the number of anti-neutrinos as  $290 \pm 69$  events/day with 1 ton prototype.

Further study is needed to consider the correlated background from muon nuclear spallation and fast neutron correlated backgrounds as next step.

### 7. Summary and discussion

We develop the Gd-doped plastic scintillator and tested with

the Am/Be pseudo anti-neutrino source. Even the sample size is small but we obtain the neutrino candidates with the delayed coincidence method. We also perform the simulation study with assuming the 1 ton size of large detector prototype and estimate the detected number of anti-neutrinos as  $292 \pm 17$  neutrinos/day.

To evaluate the actual backgrounds for the large detector, now we are developing second large prototype of Gd-doped plastic scintillator detector ( $\sim 400$  kg).

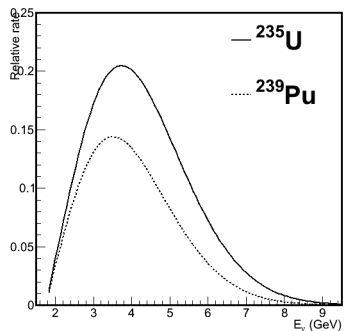


**Figure 11** Anti-neutrino energy spectra from  $^{235}\text{U}$  and  $^{239}\text{Pu}$  nuclear fission, convoluted with the inverse-beta-decay reaction cross-section

Further study for the nuclear fuel monitor, plutonium removal detection from the reactor core is crucial as a safeguard application. To detect the plutonium removal from the nuclear fuel assembly, we can indirectly measured with the anti-neutrino reduction at the nuclear fuel exchange cycle. Plutonium component produces smaller amount of anti-neutrinos than uranium in the fuel after burn-up, as shown in Figure 11. But in actual experiment, we only observe the sum spectrum from each contribution of the compound nuclear fuel assembly after burn-up. From the evolution of the nuclear fuel through the reactor operation, generated anti-neutrino flux gradually reduce from the both contributions of  $^{235}\text{U}$  reduction and  $^{239}\text{Pu}$  increase. From the fuel composition difference between the fresh and spent fuel, we will observe the growth of the anti-neutrino flux after the reactor fuel exchange. From this behavior, we can distinguish the removal of the plutonium from the reactor core indirectly via anti-neutrino flux growth. From the estimation with 1 ton size detector, we expect around the 10% reduction of detected neutrinos,  $263 \pm 16$  neutrinos/day from the spent fuel. Finally we estimate the nuclear fuel

exchange or plutonium removal sensitivity as around the 8 days observation by 1 ton size detector.

## 8. Acknowledgement

We would like to acknowledge all the member of Niigata University VND group for a good discussion in the meeting.

This study is partially supported by the Grant in Aid Scientific research JSPS fund.

## References

1. F. Reines, C.L.Cowan, "The Neutrino", Nature 178, 446 - 449 (01 September 1956)
2. IAEA Information Circular (INFCIRC)153 paragraph 28
3. BESS experiment, Physics Letters B 564 (2003) 8–20
4. Chooz experiment, Eur. Phys. J. C 27, 331–374 (2003)
5. SONGS experiment, arXiv:0808.0698v2 [nucl-ex] (2008)